Transactions of the Materials Research Society of Japan 31[4] 1029-1032 (2006)

High Strength Nanocrystalline ZrO_2–Spinel Ceramics

K. Morita, B.-N. Kim, H. Yoshida, K. Hiraga and Y. Sakka,
National Institute for Materials Science, 1-2-1 Sengen, Tsukuba, Ibaraki 305-0047
Fax: +81-29-859-2501, e-mail: MORITA.Koji@nims.go.jp

Dense nanocrystalline ZrO_2-spinel composite with average grain sizes smaller than 100 nm can successfully be fabricated by employing high-energy ball-milling and spark-plasma-sintering techniques. The fracture strength σ_f of the composite monotonously increases with a reduction of grain size. The maximum σ_f of the nanocrystalline composite with $d \approx 96$ nm reached ≈2500 MPa. As compared with that of submicrometer-sized composite with $d \approx 350$ nm, nano-crystalization can strengthen the ZrO_2-spinel composite by a factor of 2.0-2.5. The high σ_f can be associated mainly with a decrease in flaw size due to grain size reduction.

Keywords: ZrO_2, nano-composite, high-energy ball-milling, fracture strength

1. INTRODUCTION

Recently, we have attained high-strain-rate superplasticity (HSRS) in ZrO_2-spinel composite. The composite with submicrometer-sized grains of $d \approx 350$ nm exhibits a tensile elongation of 250% at strain rate of 0.7 s^{-1} and at 1823 K.[1-3] HSRS in ceramic materials have also been expected to be use for shape forming applications as in superplastic metallic alloys. For industrial application of ceramic materials, improvement of mechanical properties is also required as well as superplasticity.

For ceramic materials, reducing the grain size less than 100 nm is known to be one of the promising ways for improving the mechanical properties such as fracture toughness, fracture strength.[4-8] Nano-crystallization is also effective way for attaining HSRS because superplasticity is closely related to grain size. The present study was therefore performed to fabricate nanocrystalline ceramics with the grain sizes smaller than 100 nm by employing high-energy ball-milling (HEBM) and spark-plasma-sintering (SPS) techniques.

In this report, we lay an emphasis on the relationship between nanocrystalline structure and fracture strength of ZrO_2-30vol% spinel composite.

2. EXPERIMENTAL PROCEDURES

2.1 Material Preparation

The nanocrystalline ZrO_2-30vol% $MgAl_2O_4$ spinel composite was fabricated by employing high-energy ball-milling (HEBM) and spark-plasma-sintering (SPS) techniques as described elsewhere.[9,10] Briefly, tetragonal ZrO_2 powder (TZ-3Y, Tosoh Co., Ltd.,) mixed with 30vol% spinel powder (SP-12, Iwatani Co. Ltd.) was milled with a planetary ball-milling machine (Fritsch Co., Ltd., Germany) for 0-400 h in ethanol using ZrO_2 ball media and container. Using HEBM process, the particle size of the mixed powder can effectively be reduced to nanometer-sizes. The ball-milled powders were consolidated with a SPS machine (Sumitomo Coal Mining Co., Japan) under vacuum. By applying a load of 70 MPa, the mixed powders were rapidly heated up to 1573 K at a heating rate of about 100 °C/min and then held at the temperature for 5 min.

2.2 Mechanical Properties

Fracture strength σ_f was measured by three-point-bending test at room temperature. From the consolidated composites, rectangular bars with a cross section of 2.4 mm in width and 1.5 mm in thickness were cut out. The measurements were performed at a 16 mm span and a crosshead displacement rate of 0.5 mm/min using an Instron-type machine. Fracture strength σ_f was evaluated by the following equation:

$$\sigma_f = 3PL/2wt^2, \qquad (1)$$

where P is peak load, L is span length and w and t are width and thickness of the bending specimen, respectively.

2.3 Micrstructural Characterization

The microstructure of the SPSed specimens were characterized by X-ray diffraction (XRD), SEM and TEM. The phases of the composites were determined by X-ray diffraction (XRD) using Cu$K\alpha$ radiation operating at 40 kV and 300 mA.

For SEM observation, the surface of the specimens were mechanically polished and thermally etched at 1473 K for 10 min. The average grain size, d, was determined as 1.56 times of the average intercept lengths of grains in SEM micrographs.[11] For TEM observation,

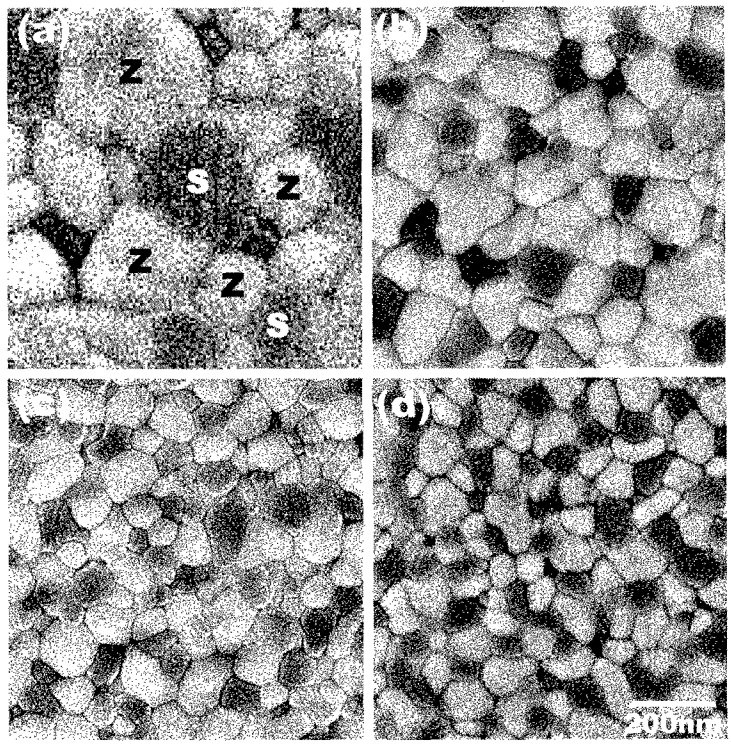

Fig. 1 Typical SEM images of ZrO_2-30vol% spinel composites; (a) pressureless-sintered in air at 1673 K for 2 h and SPSed at 1573 K for 5 min after (b) 50h, (c) 250h and (d) 400h HEBM process.

thin sheets with a thickness of about 500 μm were cut from the vicinity of fracture surfaces with a low-speed diamond cutter, mechanically polished to about 100 μm in thickness and further thinned with an Ar ion-milling machine.

3. EXPERIMENTAL RESULTS

3.1 Nanocrystalline Composite Consolidated by SPS

Figure 1(a) shows the microstructure of the ZrO_2-spinel composite pressureless-sintered in air at 1673 K for 2 h, which is conventionally used for the sintering of ZrO_2 ceramics. Under the conventional condition, although the relative density ρ of the composite reaches >98%, the average grain size d exceeds 300 nm as typically shown in Fig. 1(a).

On the other hand, the HEBM and SPS processed composites have finer and homogenous microstructure as compared with that of the composite fabricated by the conventional procedure. The grain size monotonously decreases with ball-milling time. It should be noted that, after 400 h ball-milling, the grain size reduced less than 100 nm as shown in Fig. 1(d).

In general, the powders tend to agglomerate with a reduction of the size, resulting in the formation of residual pore even after sintering. The spinel particles, however, disperse homogenously among ZrO_2 matrix and no agglomeration was found. By combining HEBM and SPS techniques, dense and nanocrystalline composite can successfully fabricated; $\rho > 98$ % and $d \approx$ 96 nm after 400h ball-milling.[10]

After pressureless-sintering and SPS processes, the XRD profile of the dense ZrO_2-spinel composite shows sharp peaks. All the detected peaks can be indexed from tetragonal (t-) ZrO_2 and spinel phases. Although a minor peak of monoclinic (m-) ZrO_2 phase was detected in the mixed powders, no peaks from m-ZrO_2 and cubic ZrO_2 phases was detected after sintering.

3.2 Fracture Strength of Nanocrystalline ZrO_2-Spinel Composite

Figure 2 shows the relationship between fracture strength σ_f and grain size d. The fracture strength monotonously increases with a reduction of grain size. For the submicrometer-sized composite with $d \approx 300$ nm, for example, an average strength is about 900 MPa. The strength is slightly lower than that of monolithic t-ZrO_2. The decrease in σ_f may be attributed to the dispersion of lower strength spinel phase; $\sigma_f \approx 250$ MPa for monolithic spinel polycrystal.[12]

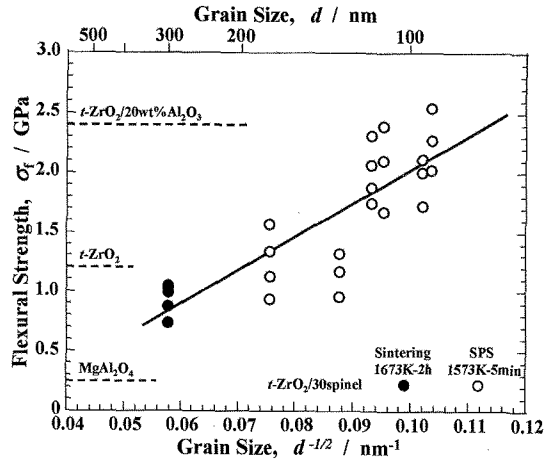

Fig. 2 Fracture strength σ_f plotted as a function of inverse square-root of grain size $d^{-1/2}$.

For the nanocrystalline composite with $d \approx 96$ nm, the average fracture strength reaches high values as high as 2200 MPa. The maximum strength of $\sigma_f \approx 2500$ MPa reached almost the same level of $\sigma_f \approx 2400$ MPa reported in ZrO_2-Al_2O_3 composite [13,14], which is classed to the highest σ_f in oxide ceramic materials. This suggests that the refinement of grain size is highly effective for strengthening the present composite. The nanocrystalization less than 100 nm can improve σ_f of the ZrO_2-spinel composite by a factor of 2.0-2.5.

3.3 Microstructural Examination

Figure 3 shows XRD profiles taken from the fracture surfaces. For submicrometer-sized composite exhibiting $\sigma_f \approx 900$ MPa, XRD analysis shows of m-ZrO_2 phase. For the high strength nanocrystalline composite exhibiting $\sigma_f \approx 2300$ MPa, on the other hand, XRD analysis shows no peaks of m-ZrO_2 phase was detected and all the detected peaks can be indexed from t-ZrO_2 and spinel phases shown in Fig. 3.

The fractured substructures were examined by TEM. The substructures were consistent well with the

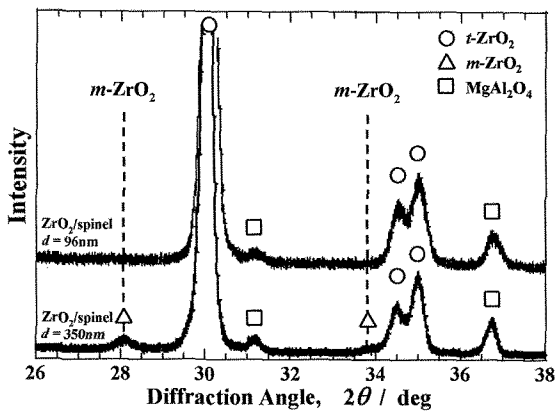

Fig. 3 XRD profiles taken from fracture surfaces of submicrometer-sized (top) and nanocrystalline (bottom) ZrO_2-30vol% spinel composites.

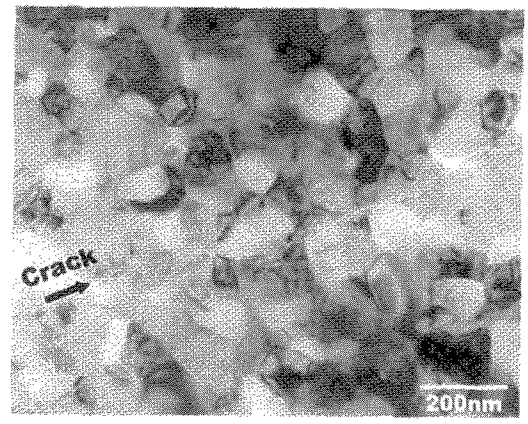

Fig.4 Typical TEM image of fractured nano-crystalline ZrO_2-30vol% spinel composite.

result of XRD. For submicrometer-sized composite, m-ZrO_2 phase was frequently observed in the grain interior. For the high strength nanocrystalline composite, however, no m-ZrO_2 phase was observed even around cracks as shown in Fig. 4. This result suggests that $t \rightarrow m$ transformation does not occur in the nanocrystalline ZrO_2-spinel composite.

4. DISCUSSION

The fracture strength, σ_f, of brittle materials can be expressed by the following equation[15-17]

$$\sigma_f \propto K_{IC}/Y a^{1/2}, \qquad (2)$$

where K_{IC} is the fracture toughness, Y is the shape factor of flaw and a is the radius of critical flaw. As expected from this relationship, fracture strength σ_f can be heightened by an increase in the fracture toughness K_{IC} or a reduction of the radius of critical flaw a.

For ZrO_2 ceramics, K_{IC} has often been related to stress-induced $t \rightarrow m$ phase transformation toughening.[17] However, XRD analysis and TEM observation show that $t \rightarrow m$ phase transformation occurs in the fracture surfaces in the submicrometer-sized composite, but not for the high strength nanocrystalline composite. For the present composite, therefore, the extremely high σ_f value would not contribute mainly to K_{IC} due to the $t \rightarrow m$ phase transformation.

According to the relation between σ_f and a in Eq. (2), a reduction of residual flaw size is effective in increasing σ_f.[18] In general, the flaw size is proportional to the grain size in dense materials. Thus, the attained dense and homogeneous nano-structure smaller than 100 nm would act as a possible factor for heightening σ_f of the present ZrO_2-spinel composite.

Since the strength of ZrO_2 ceramics is known to be closely related to microstructures such as grain size, composite system and defects,[17] additional examinations are necessary for an understanding of the

strengthening mechanism. Nevertheless, the grain size dependent flexural strength shows that a reduction in a due to nano-crystalization would be an effective way for attaining the high σ_f in the ZrO_2-spinel composite.

5. SUMMARY

The effect of nano-crystalization on the fracture strength was examined in ZrO_2-30vol% spinel composite. The fracture strength σ_f of the composite monotonously increases with a reduction of grain size. The maximum σ_f of the nanocrystalline composite with $d \approx 96$ nm reached ≈2200 MPa. As compared with that of submicrometer-sized composite with $d \approx 350$ nm, nano-crystalization can strengthen the ZrO_2-spinel composite by a factor of 2.0-2.5. The high σ_f can be associated mainly with a decrease in flaw size due to grain size reduction.

ACKNOWLEDGEMENTS

The authors are grateful to the Mitsubishi Foundation for supporting a part of the present work.

REFERENCES

[1] K. Morita, K. Hiraga and Y. Sakka, J. Am. Ceram. Soc., **85**, 1900-02 (2002).

[2] K. Morita, B.-N. Kim, K. Hiraga and Y. Sakka: Mat. Sci. Forum, **447-448**, 329-34 (2004).

[3] K. Morita, K. Hiraga, B.-N. Kim and Y. Sakka: Mater. Trans. **45**, 2073-77 (2004).

[4] K. Niihara, J. Ceram. Soc. Jpn., **99**, 974-82 (1991).

[5] M. J. Mayo and D. C. Hague, Nanostruct. Mater., **1**, 173-78 (1992).

[6] H. Kimura, Advances in Powder Metallurgy & Particulate Mater-1999 (PM2TEC '99, Vancouver), **12**, 55-61 (1999).

[7] G. D. Zhan, J. Kuntz, J. Wan and A. M. Mukherjee, Nature Mater., **2**, 38-42 (2003).

[8] G. D. Zhan, J. Kuntz, J. Wan, J. Garay and A. M. Mukherjee, J. Am. Soc., **86**, 200-2 (2003).

[9] K. Morita, B.-N. Kim, K. Hiraga and Y. Sakka, Trans. Mater. Res. Soc. Jpn., in press.

[10] K. Morita, K. Hiraga, B.-N. Kim, H. Yoshida and Y. Sakka, Scripta Mater., **53**, 1007-12 (2005).

[11] J. C. Wurst and J. A. Nelson: J. Am. Ceram. Soc., **55**, 109 (1972).

[12] O. Quénard, C.H. Laurent, A. Peigney and A. Rousset, Mat. Res. Bull., **35**, 1979 (2000).

[13] K. Tsukuma and K. Ueda, J. Am. Ceram. Soc., 68, C4 (1985).

[14] K. Tsukuma, K. Ueda, K. Matsushita and M. Shimada, J. Am. Ceram. Soc., **68**, C56 (1985).

[15] M.V. Swain and L.R.F. Rose, J. Am. Ceram. Soc., **69**, 511 (1986).

[16] A.G. Evans and R.M. Cannon, Acta Mater., **34**, 761 (1986).

[17] D.J. Green, R.H.J. Hannink and M.V. Swain, Transformation Toughening of Ceramics, CRC press (1989).

[18] F.F. Lange, J. Am. Ceram. Soc., **66**, 396 (1983).

(Received December 10, 2005;Accepted May 1, 2006)